Voltage-gated potassium channel blocker 4-aminopyridine induces glioma cell apoptosis by reducing expression of microRNA-10b-5p

Qin Ru*, Wei-ling Li, Qi Xiong, Lin Chen, Xiang Tian, and Chao-Ying Li
Wuhan Institutes of Biomedical Sciences, Jianghan University, Wuhan 430056, China

ABSTRACT **Accumulating evidence has demonstrated that voltage-gated potassium channels (Kv channels) were associated with regulating cell proliferation and apoptosis in tumor cells. Our previous study proved that the Kv channel blocker 4-aminopyridine (4-AP) could inhibit cell proliferation and induce apoptosis in glioma. However, the precise mechanisms were not clear yet. MicroRNAs (miRNAs) are small noncoding RNAs that act as key mediators in the progression of tumor, so the aim of this study was to investigate the role of miRNAs in the apoptosis-promoting effect of 4-AP in glioma cells. Using a microRNA array, we found that 4-AP altered the miRNA expression in glioma cells, and the down-regulation of miR-10b-5p induced by 4-AP was verified by real-time PCR. Transfection of miR-10b-5p mimic significantly inhibited 4-AP–induced caspases activation and apoptosis. Moreover, we verified that apoptosis-related molecule Apaf-1 was the direct target of miR-10b-5p. Furthermore, miR-10b-5p mimic significantly inhibited 4-AP–induced up-regulation of Apaf-1 and its downstream apoptosis-related proteins, such as cleaved caspase-3. In conclusion, Kv channel blocker 4-AP may exert its anti-tumor effect by down-regulating the expression of miR-10b-5p and then raised expression of Apaf-1 and its downstream apoptosis-related proteins. Current data provide evidence that miRNAs play important roles in Kv channels-mediated cell proliferation and apoptosis.**

Monitoring Editor
Kunxin Luo
University of California, Berkeley

Received: Feb 23, 2017
Revised: Feb 26, 2018
Accepted: Feb 27, 2018

INTRODUCTION

Gliomas are the most common malignant brain tumors, accounting for ~50% of all CNS tumors (Gao *et al.*, 2016). Gliomas are characterized by rapid cell growth and diffuse cellular infiltration into adjacent normal tissues (Ru *et al.*, 2012). Although surgery combined with radiotherapy plus chemotherapy improves survival, the prognosis remains poor with high recurrence rates and a median survival of only 14.6 mo (Chen *et al.*, 2016b). Therefore, understanding the mechanisms that regulate glioma growth is critical to improving the poor prognosis for patients.

An intriguing aspect of the biology of malignant glioma is that it is the same ion transport mechanisms that normally control homeostatic processes such as the regulation of cell volume and differentiation, which often become part of the pathogenesis of glioma (Thompson and Sontheimer, 2016; Lu *et al.*, 2017) The expression profile of ion channels, especially voltage-gated potassium channels (Kv channels) is known to be profoundly altered in glioma cells, and these alterations have been demonstrated to trigger relentless growth (Becchetti, 2011). For instance, Kv10.1 is highly expressed in brain metastasis and glioblastoma multiforme. Compared with those patients with high Kv10.1 expression, patients with low Kv10.1 expression had a significantly longer overall survival (Martinez *et al.*, 2015). Our previous study also proved that Kv channel blockers, such as 4-aminopyridine (4-AP) and tetraethylammonium, could inhibit cell proliferation and induce apoptosis in glioma in the concentration range required to block K_V channel currents (Ru *et al.*, 2014). However, the precise cellular mechanisms by which Kv channel activities contribute to the cell proliferation and apoptosis are not clear yet.

This article was published online ahead of print in MBoC in Press (http://www.molbiolcell.org/cgi/doi/10.1091/mbc.E17-02-0120) on March 5, 2018.

*Address correspondence to: Qin Ru (ruq.whibs@aliyun.com).

Abbreviations used: 4-AP, 4-aminopyridine; Apaf-1, apoptotic protease-activating factor 1; DMSO, dimethyl sulfoxide; FBS, fetal bovine serum; GAPDH, glyceraldehyde-3-phosphate dehydrogenase; Kv channels, voltage-gated potassium channels; miRNAs, microRNAs; MTT, 3-(4, 5-dimethylthiazol-2-yl)-2, 5-diphenyltetrazolium bromide; PARP, poly ADP-ribose polymerase; PBS, phosphate-buffered saline; qPCR, quantitative real-time PCR; RPMI-1640, Roswell Park Memorial Institute-1640; TBS, Tris-buffered saline.

MicroRNAs (miRNAs) are small noncoding RNAs that regulate gene expression through degradation of mRNA or translational inhibition of target mRNA (Bushati and Cohen, 2007). Accumulated evidence suggests that miRNAs are involved in various kinds of tumors (Liu *et al.*, 2015). MiRNAs act as key mediators in the progression and transformation of tumor by regulating of proliferation, differentiation, and apoptosis (Visone and Croce, 2009). Some miRNAs have been identified to act as oncogenes in glioma, including miR-10b (Teplyuk *et al.*, 2015, 2016; El Fatimy *et al.*, 2017), miR-149 (Shen *et al.*, 2016), and miR-106-5p (Liu *et al.*, 2014). Other miRNAs, such as miR-584-3p, have been identified to function as tumor suppressors. For example, miR-584-3p reduces the migration and invasion of human glioma cells by targeting hypoxia-induced ROCK1 (Xue *et al.*, 2016). These reports show a solid basis for the importance of miRNAs in the pathogenesis of glioma and emphasize the implications of miRNAs in diagnosis, therapy, and prognosis of glioma.

There is a growing need to uncover the complex regulatory mechanisms governing the activation and suppression of miRNA expression (Martin *et al.*, 2012), while many aspects of miRNA-induced protein regulation are known. Interestingly, alterations in expression and function of ion channels/transporters have been demonstrated to result in changes in miRNA expression (Jiang *et al.*, 2012). For example, miR-149-3p and miR-424-5p were regulated by blocking Kv channels (Ru *et al.*, 2015). Some of the miRNAs, such as miR-155, miR-21, and miR-23, were regulated by cystic fibrosis transmembrane conductance regulator, a cAMP-activated anion channel conducting both Cl^- and HCO_3^- (Bhattacharyya *et al.*, 2011). Nevertheless, further studies are still required to investigate the molecular mechanism of miRNAs in ion channels-induced anti-cancer effects.

In the current study, we have investigated the role of miRNAs in the anti-cancer effect of Kv channel blocker 4-AP in human glioma U87-MG cells and U251 cells. This may provide support for new mechanisms of Kv channels in mediating cell proliferation and apoptosis.

miRNA	Up-, down-regulation	Fold	*P* value
hsa-miR-149-3p	Up	2.01 ± 0.15	0.013
hsa-miR-1234-5p	Up	1.36 ± 0.06	0.001
hsa-miR-3196	Up	1.64 ± 0.07	0.003
hsa-miR-4291	Up	1.47 ± 0.05	0.043
hsa-miR-4281	Up	1.77 ± 0.19	0.038
hsa-miR-4488	Up	1.59 ± 0.09	0.049
hsa-miR-4497	Up	2.64 ± 0.21	0.007
hsa-miR-4646-5p	Up	2.01 ± 0.19	0.006
hsa-miR-4690-5p	Up	2.09 ± 0.66	0.044
hsa-let-7a-5p	Down	0.78 ± 0.06	0.001
hsa-let-7b-5p	Down	0.68 ± 0.06	0.043
hsa-let-7b-3p	Down	0.71 ± 0.03	0.006
hsa-let-7c	Down	0.72 ± 0.05	0.021
hsa-let-7i-5p	Down	0.75 ± 0.03	0.007
hsa-let-7d-5p	Down	0.72 ± 0.04	0.001
hsa-miR-10b-5p	Down	0.57 ± 0.06	0.001
hsa-miR-25-3p	Down	0.58 ± 0.03	0.001
hsa-miR-30c-5p	Down	0.79 ± 0.04	0.028
hsa-miR-100-5p	Down	0.60 ± 0.05	0.002

The results present fold change of signal ratio of 5 mmol/l 4-AP–treated cells to untreated control cells. The raw data were normalized and analyzed with software of MatLab version7.4, which produced an average value of the three spot replications of each miRNAs.

TABLE 1: Microarray analysis of miRNA expression in U87-MG cells treated with 5mmol/l 4-AP.

RESULTS

Effect of 4-AP on miRNA expression of glioma cells

To examine the effect of miRNAs in 4-AP–induced cell apoptosis, the μParaflo miRNA microarray containing 2042 mature human miRNA probes was used. We found that the expression of specific miRNAs in 4-AP–treated U87-MG cells was significantly altered when compared with that in untreated cells. The results are summarized in Table 1. Of the 2042 human miRNAs tested, nine miRNAs were up-regulated and 10 miRNAs were down-regulated in our experiment. Based on previously published reports (Gabriely *et al.*, 2011; Lin *et al.*, 2012; Teplyuk *et al.*, 2015), we selected the down-regulated miR-10b-5p and verified its expression level by real-time PCR. Compared with untreated control cells, real-time PCR data confirmed that the expression of miR-10b-5p was down-regulated significantly in the 4-AP–treated U87-MG cells (Figure 1C). To test whether these results were also present in other glioma cells, we chose another glioma cell line to examine the effect of 4-AP on proliferation, apoptosis, and expression of miR-10b-5p in U251 cells. As shown in Figure 1, 4-AP treatment within a certain concentration range significantly inhibited the cell proliferation of U251 cells (Figure 1A) and resulted in a markedly activation of caspase-3 (Figure 1B). In real-time PCR assay, the expression of miR-10b-5p was also down-regulated significantly in the 4-AP–treated U251 cells comparing with untreated control cells (Figure 1D). On the other hand, treatment of low-passage HEK293 cells with the same doses of 4-AP demonstrated the effects of 4-AP on cell proliferation, apoptosis, and miR-10b-5p expression in glioma cells were less evident in low-tumorigenicity cells (Supplemental Figure S1).

Effect of miR-10b-5p on the proliferation of glioma cells

Previous reports have shown that miR-10b-5p acted as a promoter of cell growth in glioma (Gabriely *et al.*, 2011; Lin *et al.*, 2012; Lu *et al.*, 2014; Teplyuk *et al.*, 2015). To determine the role of miR-10b-5p in the proliferation of glioma cells, the 3-(4, 5-dimethylthiazol-2-yl)-2, 5-diphenyltetrazolium bromide (MTT) assay was used after transfection of miR-10b-5p mimic, inhibitor, and negative control in U87-MG cells and U251 cells. As shown in Figure 2, compared with the corresponding control, overexpression of miR-10b-5p significantly promoted the proliferation of U87-MG cells at 48 h (Figure 2A), and miR-10b-5p inhibitor dramatically inhibited cell proliferation at 48 h (Figure 2B). No apparent changes in cell survival were detected at 24 h. Similar results were found in U251 cells (Figure 2, C and D).

MiR-10b-5p is involved in 4-AP–induced growth inhibition in glioma cells

Given that miR-10b-5p has been confirmed to promote glioma cell proliferation, we sought to further investigate its role in 4-AP–induced cytotoxicity. MiR-10b-5p mimic, inhibitor, and negative control were transfected into U87-MG cells and U251 cells. As shown in Figure 3, miR-10b-5p mimic significantly increased the proliferation of U87-MG cells treated with 4-AP compared with the

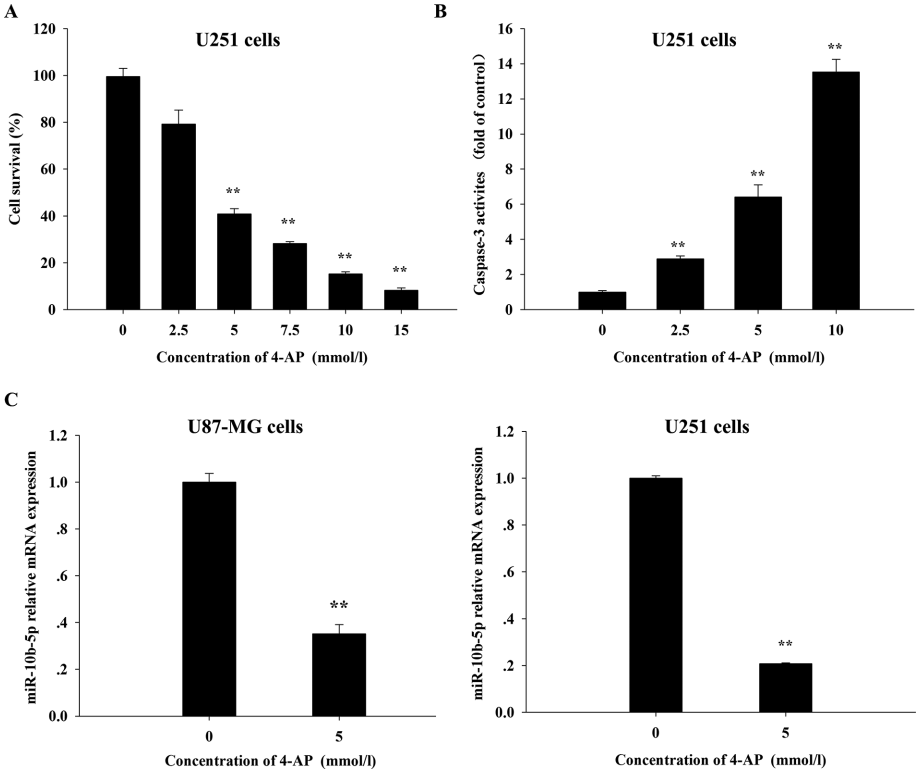

FIGURE 1: Effect of 4-AP on proliferation, apoptosis, and miRNAs expression in glioma cells. U251 cells were treated with 4-AP for 24 h at the indicated concentrations, and cell proliferation assay (A) and caspase-3 activities assay (B) were performed as described under *Materials and Methods*. Cell proliferation experiment was performed in triplicate and repeated three times in cells pertaining to different passages. Caspase-3 activities assay was repeated three times in cells pertaining to different passages. The expressions of miR-10b-5p in U87-MG cells (C) and U251 cells (D) treated with 5 mM 4-AP were verified by real-time PCR. The results of real-time PCR present fold change of miR-10b-5p expression in 5 mM 4-AP treated cells to untreated control cells. Fold change of miR-10b-5p expression is presented in $2^{-\Delta\Delta Ct}$. Each set of experiments was performed in triplicate. $^{**}p < 0.01$, compared with the untreated control cells.

cells transfected with mimic control and treated with 4-AP. The cell survival rate of group treated with mimic control and 4-AP was 53.31 ± 2.24%, while that of group treated with mimic and 4-AP was 63.31 ± 2.19% (Figure 3A). Conversely, miR-10b-5p inhibitor significantly decreased the proliferation of U87-MG cells treated with 4-AP compared with the cells transfected with inhibitor control and treated with 4-AP (Figure 3B). Similar results were observed in U251 cells (Figure 3, C and D).

MiR-10b-5p is involved in 4-AP–induced cell apoptosis in glioma cells

4-AP was known to exert its tumor growth inhibitory effect through the induction of apoptosis (Ru *et al.*, 2014). We further examined whether miR-10b-5p involve in 4-AP–induced cell apoptosis in glioma cells. The rate of apoptosis was measured by a Muse Cell Analyzer following 4-AP treatment. Transfection of the miR-10b-5p mimic significantly prevented 4-AP–induced apoptosis in U87-MG cells, as compared with the cells transfected with mimic control and treated with 4-AP. The percentage of apoptotic cells in group treated with mimic control and 4-AP was 18.83 ± 0.59%, while that of group treated with mimic and 4-AP was 10.78 ± 0.58% (Figure 4, A and B). Conversely, the miR-10b-5p inhibitor significantly accelerated 4-AP–induced apoptosis in U87-MG cells. The percentage of apoptotic cells in group treated with inhibitor control and 4-AP was 25.14 ± 2.56%, while that of the group treated with inhibitor and 4-AP was 34.82 ± 0.56% (Figure 4, C and D).

MiR-10b-5p is involved in 4-AP–induced mitochondria dysfunction in glioma cells

Mitochondrial membrane potential ($\Delta\Psi m$) is a key indicator of mitochondrial function, and the loss of $\Delta\Psi m$ is an indicator for mitochondrial dysfunction and a hallmark for apoptosis. Figure 5, A and B, shows that total depolarization of mitochondria in the group treated with mimic control and 4-AP was 22.34 ± 1.58%, while that in the group treated with mimic and 4-AP was 15.82 ± 0.68%. These results indicated that a significant dissipation of $\Delta\Psi m$ was triggered following 4-AP treatment and transfection of miR-10b-5p mimic significantly prevented this process. In contrast, the miR-10b-5p inhibitor significantly accelerated 4-AP–induced mitochondria dysfunction in U87-MG cells (Figure 5, C and D). Similar results were observed in U251 cells (Figure 5, E and F).

MiR-10b-5p is involved in 4-AP induction of caspase activities in glioma cells

To assess whether miR-10b-5p low expression is involved in 4-AP–induced caspase activation in glioma cells, caspase-3 and caspase-9 activities were measured after the cells were treated with 4-AP alone or 4-AP plus miR-10b-5p mimic (or inhibitor). Results from the colorimetric assay demonstrated that miR-10b-5p mimic significantly inhibited 4-AP–induced caspase-3 and caspase-9 activation in U87-MG cells compared with cells treated with 4-AP plus mimic control. The caspase-3 and caspase-9 in the group treated with mimic control plus 4-AP increased to 3.68 ± 0.05 and 6.97 ± 0.09 fold of untreated cells, while that in the group treated with mimic and 4-AP was 1.89 ± 0.10 and 3.03 ± 0.23, respectively (Figure 6, A and B). In addition, the miR-10b-5p inhibitor significantly accelerated 4-AP–induced caspase-3 and caspase-9 activation in U87-MG cells (Figure 6, C and D). In U251 cells, similar results were observed. The miR-10b-5p mimic significantly inhibited 4-AP–induced caspase-3 activation, and the miR-10b-5p inhibitor significantly accelerated 4-AP–induced caspase-3 activation (Figure 6, E and F).

Apaf-1 is a direct target of miR-10b-5p in glioma cells

Since Apaf-1 was a binding target of miR-10b-5p predicted by the online database (MicroCosm), we performed real-time PCR and Western blotting to observe the expression of Apaf-1 on mRNA and protein level in glioma cells transfected with miR-10b-5p mimic or inhibitor. As shown in Figure 7 (B and C), the mRNA level of Apaf-1 was decreased after up-regulation of miR-10b-5p and evidently increased after down-regulation of miR-10b-5p both in U87-MG cells and U251 cells. Western blotting assay showed that the protein level of Apaf-1 decreased remarkably after up-regulation of miR-10b-5p and evidently increased after down-regulation

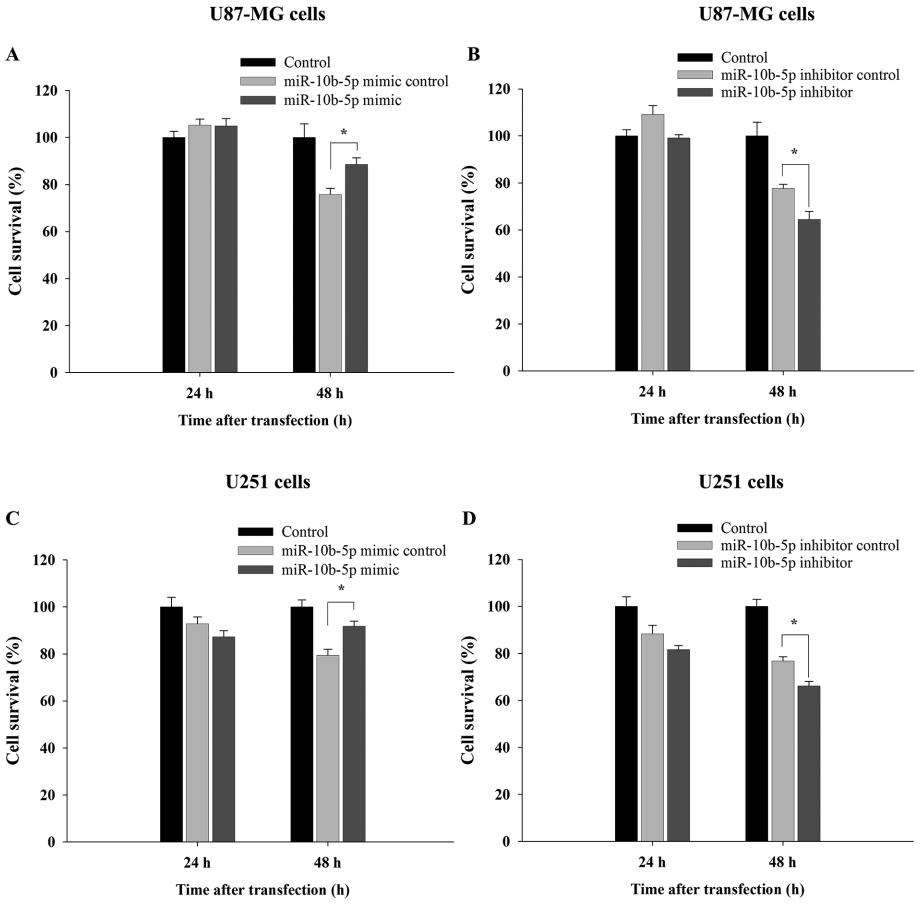

FIGURE 2: Effect of miR-10b-5p on cell proliferation in glioma cells. (A) Effect of miR-10b-5p mimic or mimic control on cell proliferation in U87-MG cells. (B) Effect of miR-10b-5p inhibitor or inhibitor control on cell proliferation in U87-MG cells. (C) Effect of miR-10b-5p mimic or mimic control on cell proliferation in U251 cells. (D) Effect of miR-10b-5p inhibitor or inhibitor control on cell proliferation in U251 cells. U87-MG cells or U251 cells were transfected with miR-10b-5p mimic or inhibitor for different time, and cell proliferation was assessed by MTT assay as described under *Materials and Methods*. Each set of experiments was performed in triplicate and repeated three times in cells pertaining to different passages. *$p < 0.05$ compared with the group transfected with corresponding control.

of miR-10b-5p in both U87-MG cells and U251 cells (Figure 7, D–G).

To further demonstrate whether Apaf-1 was a direct target of miR-10b-5p, Apaf-1 3′-UTR was cloned into a luciferase reporter vector, and the putative miR-10b-5p binding site in the Apaf-14 3′-UTR was mutated (Figure 7A). The effect of miR-10b-5p was determined using a luciferase reporter assay in HEK293 cells. The results showed that overexpression of miR-10b-5p significantly inhibited the luciferase activity of pmiR-RB-Repor-Apaf-1-3′UTR WT (Figure 7H). Mutation of the miR-10b-5p binding site in the Apaf-1 3′-UTR abolished this effect of miR-10b-5p, which suggested that Apaf-1 was directly and negatively regulated by miR-10b-5p.

The effects of miR-10b-5p and 4-AP on the expressions of apoptosis-related proteins in U87-MG cells

To investigate the possible mechanism of miR-10b-5p involved in 4-AP–induced cell apoptosis, the expression of several apoptosis-related molecules was measured. As shown in Figure 8, compared with that in the control group, the protein expression of apoptotic protease-activating factor 1 (Apaf-1), cleaved caspase-3, cleaved caspase-9, and cleaved poly ADP-ribose polymerase (PARP) was significantly increased in U87-MG cells treated by 5 mmol/l 4-AP in U87-MG cells. The mimic of miR-10b-5p significantly inhibited 4-AP–induced up-regulation of Apaf-1, cleaved caspase-3, cleaved caspase-9, and cleaved PARP. On the contrary, miR-10b-5p inhibitor significantly accelerated 4-AP–induced up-regulation of the above protein in U87-MG cells.

DISCUSSION

Since the late 2000s, accumulating evidence has indicated that Kv channels play important roles in the onset, proliferation, and malignant progression of various types of cancer (Becchetti, 2011; Lastraioli *et al.*, 2015), and Kv channel blockers have been shown to inhibit cell proliferation and induce apoptosis of cancer cells (Spitzner *et al.*, 2007). Many miRNAs have been reported to have an oncogenic or a tumor suppressor function and to be involved in cell proliferation, growth, and apoptosis (Kosik and Krichevsky, 2005; Visone and Croce, 2009). However, little is known about the relationship between miRNAs expression and the anti-tumor effect of Kv channel blockers. The present study demonstrated that 4-AP, a Kv channel blocker, altered miRNA expression in human glioma U87-MG cells, including nine up-regulated and 10 down-regulated miRNAs. Among the down-regulated miRNAs, some have been already reported to be act as an oncomiR. For instance, miR-365a-3p and miR-10b-5p function as oncomiR and may promote growth and metastasis of tumor (Teplyuk *et al.*, 2015; Geng *et al.*, 2016). On the contrary, other miRNAs up-regulated by 4-AP have been reported to be tumor suppressors, such as miR-3196, which was significantly down-regulated in basal cell carcinoma compared with nonlesional skin (Sand *et al.*, 2012). Our findings indicated that miRNAs might play important roles in the anti-tumor effect of 4-AP in glioma cells, and we continued to investigate the role of specific miRNAs in the following experiments.

Initially found to be an oncogene in metastatic breast cancer (Ma *et al.*, 2007), miR-10b appeared to play a growth-promoting role in a broad range of different cancers, including glioma, lung, pancreatic, hepatic, thyroid, gastric, and colorectal (Gabriely *et al.*, 2011; Lu *et al.*, 2014; Ouyang *et al.*, 2014; Teplyuk *et al.*, 2015; Li *et al.*, 2016). It is overexpressed in 90% of glioma tumors across all four subtypes, while it is undetectable in normal brain tissues (Teplyuk *et al.*, 2015). Inhibition of miR-10b is deleterious for glioma cells (Gabriely *et al.*, 2011). Teplyuk *et al.* proved that miR-10b regulated a major transcription factor, E2F1, driving cell-cycle progression through the S-phase and thus promoting proliferation (Teplyuk *et al.*, 2015). In our study, we found that 4-AP decreased the expression of miR-10b-5p, mature sequence of miR-10b, using microRNA array in U87-MG cells, and the down-regulation of miR-10b-5p was verified by real-time PCR in both U87-MG cells and U251 cells. To further investigate the role of miR-10b-5p in 4-AP's anti-cancer effect, miR-10b-5p mimic or inhibitor was used. Our study

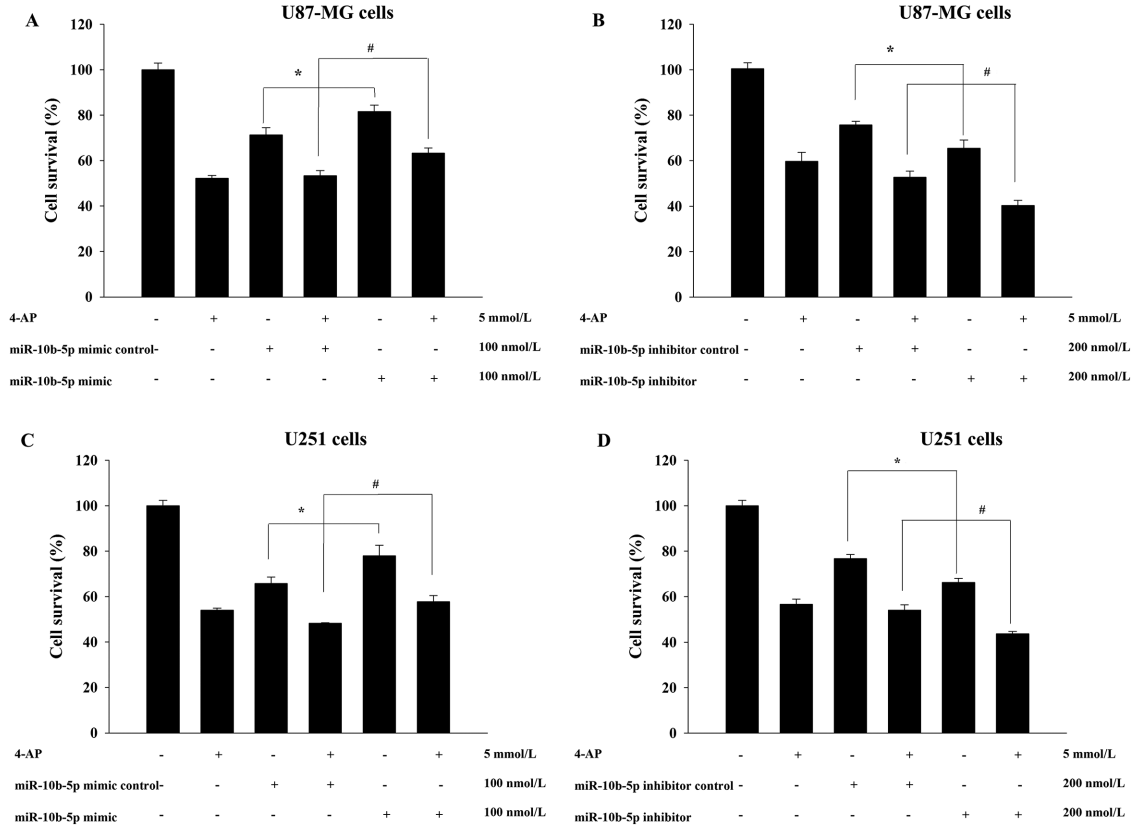

FIGURE 3: Transfection of miR-10b-5p inhibitor prevented 4-AP–induced cytotoxicity in glioma. (A) MiR-10b-5p mimic significantly increased the proliferation of U87-MG cells treated with 4-AP. (B) MiR-10b-5p inhibitor significantly decreased the proliferation of U87-MG cells treated with 4-AP. (C) MiR-10b-5p mimic significantly increased the proliferation of U251 cells treated with 4-AP. (D) MiR-10b-5p inhibitor significantly decreased the proliferation of U251 cells treated with 4-AP.U87-MG cells or U251 cells were transfected with miR-10b-5p mimic or inhibitor to up-regulate or down-regulate miR-10b-5p. At 48 h after transfection, the cells were treated with 5 mM 4-AP for 24 h. Cell proliferation was determined using the MTT assay. Each set of experiments was performed in triplicate and repeated three times in cells pertaining to different passages. $^{*}p < 0.05$, compared with cells transfected with corresponding control; $^{\#}p < 0.05$, compared with cells transfected with corresponding control and treated with 4-AP.

demonstrated that up-regulation of miR-10b-5p promoted proliferation and down-regulation of miR-10b-5p inhibited proliferation in both U87-MG cells and U251 cells. These results were consistent with previous reports (Huang *et al.*, 2015; Teplyuk *et al.*, 2015). Moreover, we found that miR-10b-5p mimic significantly restored cell viability in 4-AP–treated cells, and miR-10b-5p inhibitor significantly accelerated cell damage in 4-AP–treated cells, implying that 4-AP may play its anti-proliferative effect in glioma cells by down-regulating the expression of miR-10b-5p.

Activation of apoptotic pathways is a key mechanism by which chemotherapeutic drugs kill cancer cells. Our previous study demonstrated that 4-AP could induce apoptosis in glioma cells (Ru *et al.*, 2014), and the data in the current study confirmed that activities of caspase-3 and caspase-9 increased after 4-AP treatment in U87-MG cells, so we continued to investigate the role of miR-10b-5p in 4-AP induced cell apoptosis. Results showed that miR-10b-5p mimic significantly inhibited cell apoptosis and caspase activation in 4-AP–treated cells, and miR-10b-5p inhibitor significantly accelerated 4-AP–induced apoptosis and caspase activation in both U87-MG cells and U251 cells. These results were consistent with the results of previous studies, which proved that silencing of miR-10b promoted apoptosis and up-regulated of apoptosis-inducing member caspase-3 in NSCLC cells and endometrial cancer cells (Huang *et al.*, 2015; Chen *et al.*, 2016a). Combining with cell proliferation experiment results, we speculated that down-regulation of miR-10b-5p may be a key mechanism in 4-AP's anti-cancer effect in glioma cells.

We further analyzed the putative target genes of the miR-10b-5p and the functional relationship between the gene and anti-cancer properties using bioinformatic tools, since the cellular functions of miRNAs are directly mediated by controlling their target gene expression. The miRBase target database tool, MicroCosm, revealed that the Apaf-1 may be a direct target of miR-10b-5p. As a result, the real-time PCR, Western blotting, and luciferase reporter assay demonstrated that Apaf-1 is indeed a direct target of miR-10b-5p. Once mitochondria are permeabilized, the execution phase of apoptosis is initiated by the release of cytochrome c and activates Apaf-1 in the cytosol, and activated Apaf-1 can recruit the inactive pro-form of caspase-9 (Charles and Rehm, 2014). Importantly, we also found that miR-10b-5p inhibitor significantly induced activation of caspase-3 and caspase-9. Thus, we confirmed that miR-10b-5p played critical roles in the cell apoptosis in giloma cells, partially by down-regulating the protein expression of Apaf-1.

It is known that cell apoptosis are regulated by numerous proteins. To confirm the possible mechanism that miR-10b-5p mediated in 4-AP–induced apoptosis in U87-MG cells, we investigated

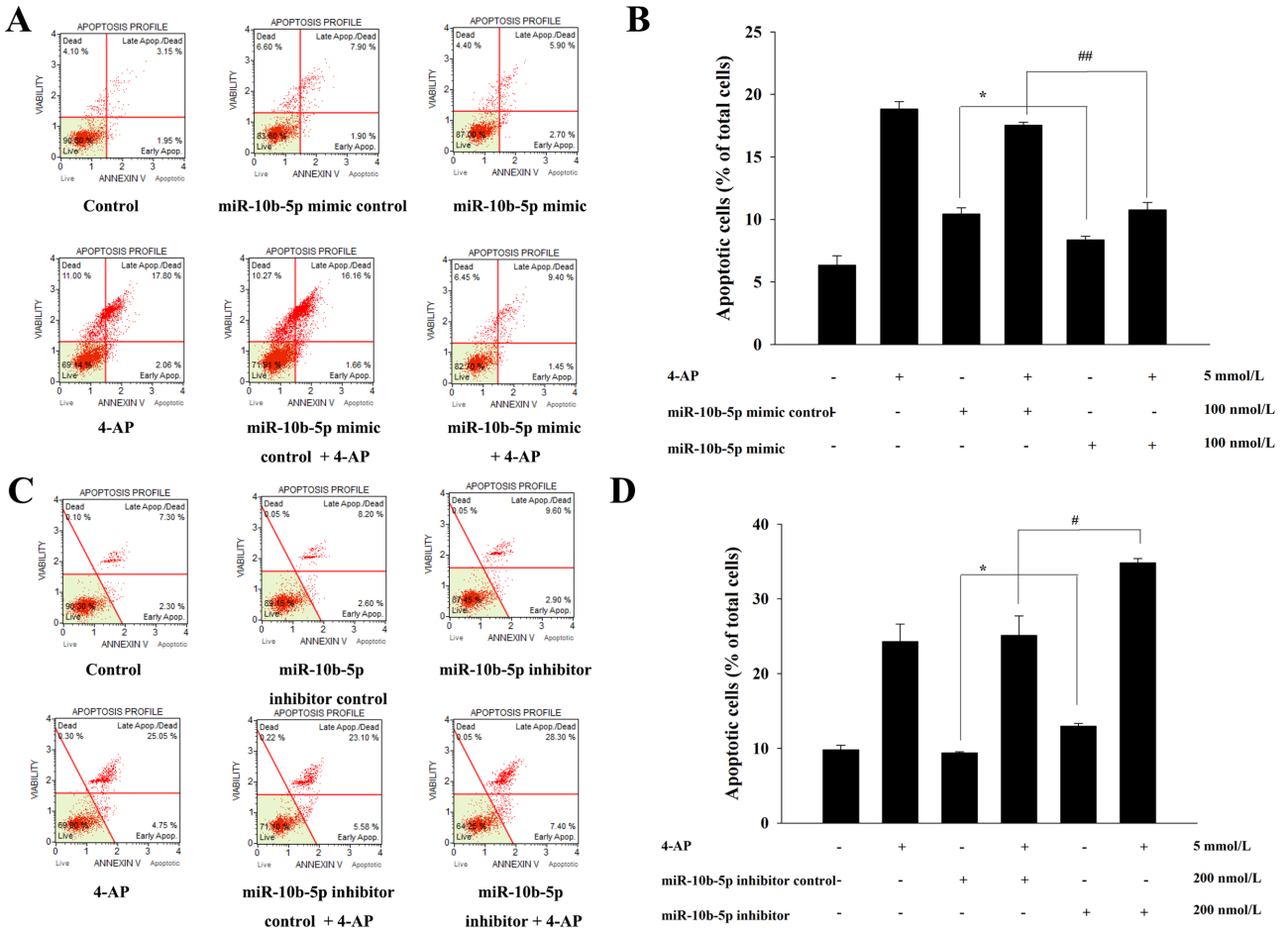

FIGURE 4: Transfection of miR-10b-5p inhibitor prevented 4-AP–induced cell apoptosis in glioma U87-MG cells. MiR-10b-5p mimic significantly prevented 4-AP–induced apoptosis in U87-MG cells. (A) A representative dot plots in live, early apoptotic, late apoptotic/dead and dead phase is shown. (B) The mean percentage of the apoptotic cells is expressed by a histogram. MiR-10b-5p inhibitor significantly accelerated 4-AP–induced apoptosis. (C) Representative dot plots in live, early apoptotic, late apoptotic/dead, and dead phases are shown. (D) The mean percentage of the apoptotic cells is expressed by a histogram. Each set of experiments was repeated three times in cells pertaining to different passages. $^{*}p < 0.05$, compared with cells transfected with corresponding control; $^{\#\#}p < 0.01$, compared with cells transfected with corresponding control and treated with 4-AP.

the effects of miR-10b-5p mimic or inhibitor plus 4-AP on apoptosis related proteins. We detected the expression of Apaf-1, cleaved caspase-3, cleaved caspase-9, and cleaved PARP. From our data, we found that the expression of Apaf-1, cleaved caspase-3, cleaved caspase-9, and cleaved PARP increased after 4-AP treatment in U87-MG cells. Further results showed miR-10b-5p mimic significantly prevented 4-AP–induced up-regulation of apoptosis related proteins in U87-MG cells, while the miR-10b-5p inhibitor significantly accelerated 4-AP–induced elevation of apoptosis related proteins. Based on these results, a series of events might occur in the procedure of the apoptotic pathway: blocking of Kv channels, down-regulation of miR-10b-5p, increasing expression of Apaf-1, formation of tetramer (composed of caspase-9, Apaf-1, cytochrome *c*, and dATP), autocatalytic activation of caspase-9, and activation of effector caspases including caspase-3 and PARP.

The mitochondrial membrane potential ($\Delta\Psi m$) is considered to be an essential step toward apoptosis, since it induces the opening of the permeability transition pore, leading to cell death by activating apoptotic signaling and caspase activities (Voloboueva and Giffard, 2011). We also found that the depolarization of $\Delta\Psi m$ increased after 4-AP treatment in U87-MG cells and U251 cells, and miR-10b-5p mimic significantly prevented 4-AP–induced mitochondria dysfunction. These results suggested that except for up-regulation of Apaf-1, down-regulation of miR-10b-5p may also induce mitochondrial dysfunction and finally contribute to 4-AP–induced cell apoptosis. However, there are no reports in the literature about the mechanism by which miR-10b-5p induces mitochondrial dysfunction. Geiger and Dalgaard (2017) reported that some miRNAs, called mitomiRs, have been found localized in mitochondrial fractions instead of the cytosol or the nucleus, including miR-99, one member of the miR-10 family. These mitomiRs may affect mitochondrial function through influencing electron transport chain, tricarboxylic acid cycle, and amino acid metabolism or mitochondrial fusion. For instance, miR-106b and the mitomiR miR-140 have been implicated with mitochondrial dysfunction and contributed to apoptosis through targeting mitofusin 1 and mitofusin 2 (Zhang *et al.*, 2013; Li *et al.*, 2014). MicroCosm revealed that the mitofusin 1 is a direct target of miR-10b-5p, suggesting that miR-10b-5p might influence the expression of mitofusin 1, affect mitochondrial function, and participate in 4-AP–induced cell apoptosis. Further studies are

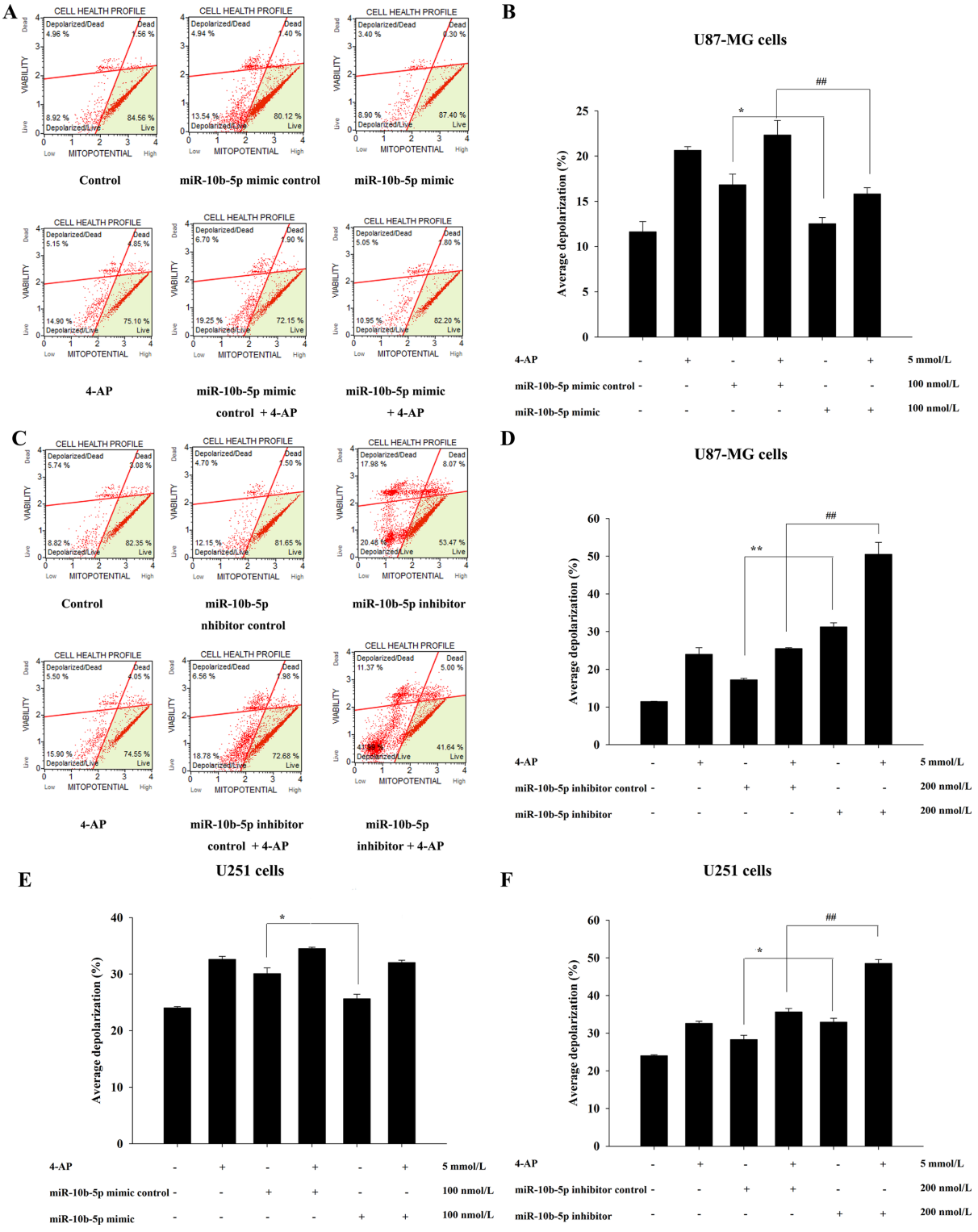

FIGURE 5: Transfection of miR-10b-5p inhibitor prevented 4-AP–induced mitochondria dysfunction in glioma cells. (A) MiR-10b-5p mimic significantly prevented 4-AP–induced mitochondria dysfunction in U87-MG cells. Representative dot plots in live, depolarized/live, depolarized/dead, and dead phase are shown. (B) The mean percentage of the total depolarization is expressed by a histogram. (C) MiR-10b-5p inhibitor significantly accelerated 4-AP–induced mitochondria dysfunction in U87-MG cells. Representative dot plots in live, depolarized/live, depolarized/dead, and dead phases are shown. (D) The mean percentage of the apoptotic cells is expressed by a histogram. (E) MiR-10b-5p mimic significantly prevented 4-AP–induced mitochondria dysfunction in U251 cells. (F) MiR-10b-5p inhibitor significantly accelerated 4-AP–induced mitochondria dysfunction in U251 cells. Each set of experiments was repeated three times in cells pertaining to different passages. *$p < 0.05$, **$p < 0.01$, compared with cells transfected with corresponding control; $^{\#\#}p < 0.01$, compared with cells transfected with corresponding control and treated with 4-AP.

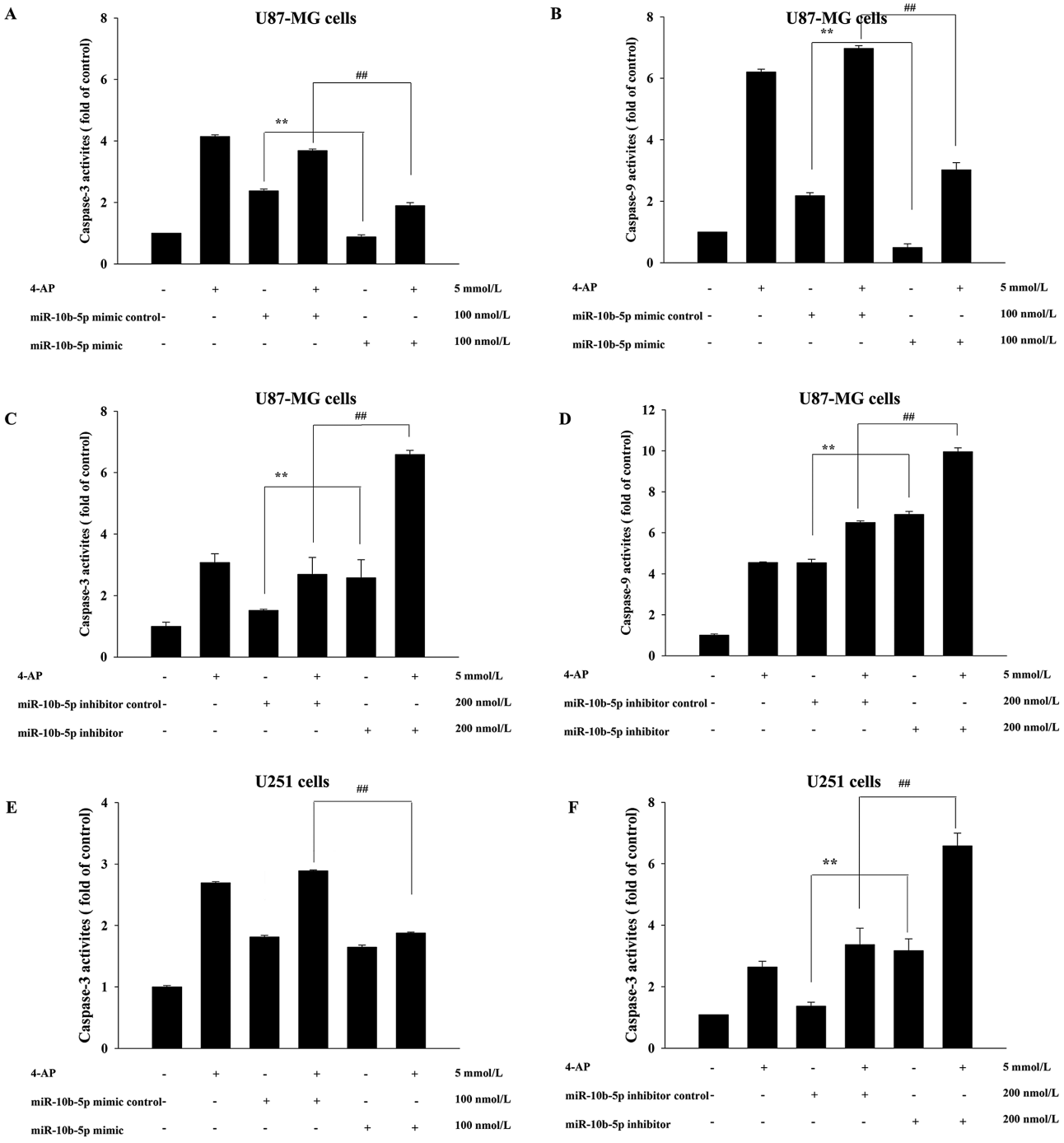

FIGURE 6: Transfection of miR-10b-5p inhibitor prevented 4-AP–induced caspase activation in glioma U87-MG cells. MiR-10b-5p mimic significantly inhibited 4-AP–induced caspase-3 (A) and caspase-9 (B) activation in U87-MG cells. MiR-10b-5p inhibitor significantly accelerated 4-AP–induced caspase-3 (C) and caspase-9 (D) activation in U87-MG cells. (E) The miR-10b-5p mimic significantly inhibited 4-AP–induced caspase-3 activation in U251 cells. (F) The miR-10b-5p inhibitor significantly accelerated 4-AP–induced caspase-3 activation in U251 cells. Each set of experiments was repeated three times in cells pertaining to different passages. $^{**}p < 0.01$, compared with cells transfected with corresponding control; $^{\#\#}p < 0.01$, compared with cells transfected with corresponding control and treated with 4-AP.

still required to elucidate the relationship between miR-10b-5p and mitochondrial dysfunction.

In conclusion, the present study showed that miR-10b-5p inhibited apoptosis of glioma cells through directly targeting Apaf-1, activating the caspase signaling pathway, and Kv channel blocker 4-AP may exert its anti-cancer effect in glioma cells in part by down-regulation of miRNA-10b-5p. This finding provides new insight into the understanding of the molecular mechanism of Kv channel-mediated cytotoxicity of glioma. In addition, there are 18 miRNAs whose expression was altered after 4-AP treatment in U87-MG cells except miRNA-10b-5p; further studies are still needed to clarify the comprehensive mechanism of other miRNAs in the anti-cancer effect of Kv channel blocker 4-AP in human glioma cells.

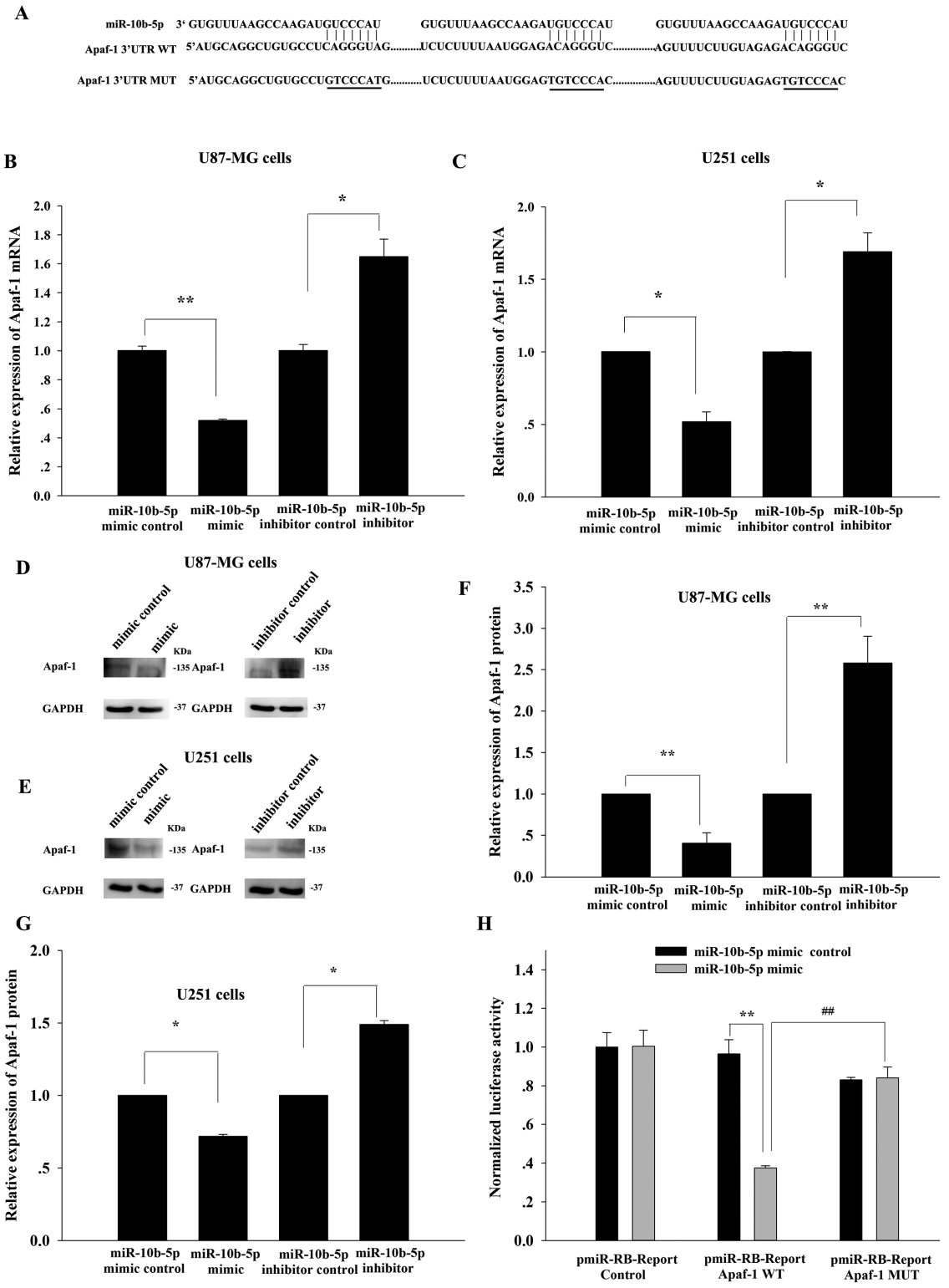

FIGURE 7: Apaf-1 is a direct target of miR-10b-5p. (A) Schematic representation of Apaf-1 3'UTRs showing putative miR-10b-5p target site. The mRNA expression of Apaf-1 was determined by real-time PCR in U87-MG cells (B) and in U251 cells (C). GAPDH was detected as endogenous control. Each set of experiments was performed in triplicate. The protein expression of Apaf-1 was determined by Western blotting in U87-MG cells (D, F) and in U251 cells (E, G). Each set of experiments was repeated three times in cells pertaining to different passages. *$p < 0.05$, **$p < 0.01$, compared with the group transfected with corresponding control. (H) The analysis of the relative luciferase activities of Apaf-1 WT, Apaf-1 MUT in HEK293 cells. The experiment was performed in triplicate. *$p < 0.05$, **$p < 0.01$, compared with cells transfected with corresponding control, ##$p < 0.01$, compared with cells transfected with Apaf-1 WT.

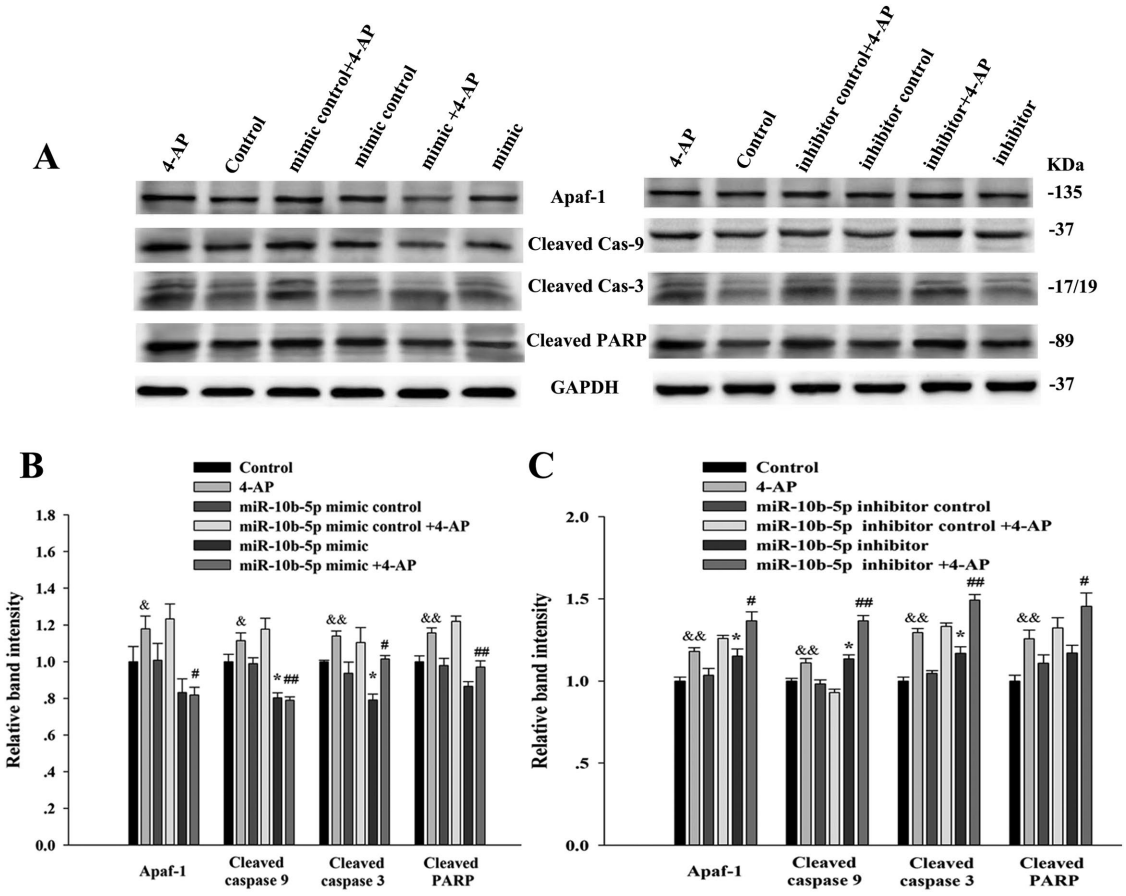

FIGURE 8: The effects of miR-10b-5p and 4-AP on the expressions of apoptosis-related proteins in glioma cells. (A) The expressions of Apaf-1, cleaved caspase-3, cleaved caspase-9, and cleaved PARP were determined by Western blotting in U87-MG cells. (B, C) The relative expression of Apaf-1, cleaved caspase-3, cleaved caspase-9, and cleaved PARP were determined in U87-MG cells. GAPDH was detected as endogenous control. Each set of experiments was repeated three times in cells pertaining to different passages. $^{\&}p < 0.05$, $^{\&\&}p < 0.01$, compared with control cells; $^{*}p < 0.05$, compared with cells transfected with corresponding control; $^{\#}p < 0.05$, $^{\#\#}p < 0.01$, compared with cells transfected with corresponding control and treated with 4-AP.

MATERIAL AND METHODS

Chemicals and materials

4-Aminopyridine (4-AP) and MTT were products of the Sigma Chemical Corp. (St. Louis, MO). Roswell Park Memorial Institute-1640 (RPMI-1640) medium, DMEM, and fetal bovine serum (FBS) were obtained from Life Technologies (Carlsbad, CA). Muse Annexin V and the Dead Cell Kit (MCH100105) and the Muse MitoPotential Kit (MCH100110) were procured from Millipore Corporation (Darmstadt, Germany). The caspase-3 activity assay kit (C1116), caspase-9 activity assay kit (C1158), and mycoplasma Stain Assay Kit (C0296) were obtained from Beyotime Institute of Biotechnology (Haimen, China). Protein extraction buffer (AR0105), protease (AR1182), and phosphatase inhibitors (AR1183) were obtained from Wuhan Boster Biological Engineering Co., Ltd (Wuhan, China). Antibodies against glyceraldehyde-3-phosphate dehydrogenase (GAPDH) (5174S), Apaf-1 (8969S), cleaved caspase-3 (9664S), cleaved caspase-9 (7237S), and cleaved PARP (5625S) were purchased from Cell Signaling Technology (Beverly, MA), and the antibodies were validated by the manufacturer. The miR-10-5p mimic, inhibitor, and negative control; pmiR-RB-Report control plasmid; pmiR-RB-Repor-Apaf-1-3′UTR wild-type plasmid; and mutant reporter plasmid were synthesized and purified by Guangzhou RiboBio Co., Ltd (Guangzhou, China). All other chemicals were of standard analytical grade.

Cell culture

Human glioma U87-MG cells, U251 cells, and human embryonic kidney 293 (HEK 293) cells (passage 40–45) (Shen *et al.*, 2008) were purchased from a typical culture preservation commission cell bank (Chinese Academy of Sciences, Shanghai, China). U87-MG cells were grown in RPMI-1640 supplemented with 10% FBS and 100 U penicillin/ streptomycin in 5% CO_2 at 37°C. U251 cells and HEK 293 cells were grown in DMEM supplemented with 10% FBS and 100 U penicillin/streptomycin in 5% CO_2 at 37°C. Cells were passaged every 3 d and maintained at exponential growth. All cell lines have been identified and were routinely screened for mycoplasma contamination using the Mycoplasma Stain Assay Kit.

Microarray analysis of miRNA gene expression

After treatment with 5 mmol/l 4-AP for 24 h, U87-MG cells were harvested in phosphate-buffered saline (PBS) and collected by centrifugation, and total RNA extracted using the miRNeasy kit (Qiagen) according to manufacturer's protocol. The experiment was repeated three times. Quantity and quality of RNA was determined by absorbance (260, 280 nm). LC Sciences (Houston, TX) performed a microarray assay using 5 μg total RNA, which was size fractioned using a YM-100 Micron centrifugal filter (Millipore), and the small RNAs (<300 nucleotides) isolated were 3′-extended with a poly(A)

tail, using poly(A) polymerase. Three biological samples of RNA were pooled, and an array was performed using quadruplicate internal repeats of pooled RNA and as previously described (Ru *et al.*, 2015). Data were analyzed by first subtracting the background, and normalization of array was to the statistical mean of all detectable transcripts. System-related variation of data was corrected using the LOWESS filter (locally weighted regression) method. Probes were single channel, and detected signals greater than background plus 3 times the SD was derived.

Quantitative real-time PCR for miRNA expression

To confirm the miRNA level obtained from the microarray results, miRNA expression was assessed using real-time PCR. The following primers were used: miR-10b-5p forward, 5′- CGGCGGATACCCTGTAGAAC-3′, reverse, 5′-GGCTG TCGTGGACTGCG-3′; RNU6B forward, 5′-CAAATTCGTGAAGCGTTCCATA-3′, reverse, 5′-AGTGCA GGGTCCGAGGTATTC-3′. RNU6B was taken as an internal control. Real-time PCR was performed using Platinum SYBR Green quantitative real-time PCR (qPCR) SuperMix-UDG (Invitrogen). The reactions were carried out in a 96-well optical plate at 95°C for 10 min and then amplified for 15 s at 90°C followed by 30 s at 60°C for 40 cycles. The relative value of miRNA was calculated using the $2^{-\Delta\Delta Ct}$ method, where Ct is the number of cycles at which the application reaches a threshold, as determined by SDS software v1.2 (Applied Biosystems). Each reverse transcription and qPCR assay was performed in triplicate.

Transient transfection

U87-MG cells and U251 cells were seeded on 96-well plates or six-well plates before transfection and incubated until 90% confluency was reached. The miR-10b-5p mimic and negative control of mimic were transfected at a final concentration of 100 nmol/l for 48 h using Lipofectamine 2000 (Life Technologies, Carlsbad, CA) according to the manufacturer's instructions. MiR-10b-5p inhibitor and negative control were transfected at a final concentration of 200 nmol/l. After transfection, the cells were treated with 4-AP for 24 h to study cell proliferation, apoptosis, as well as caspase activities and protein expression.

MTT cell proliferation assay

Briefly, cells were seeded at 5000 cells/well into a 96-well plate and incubated overnight. After exposure to different treatments, MTT solution (final concentration 0.5 mg/ml) was added to each well, and the samples were incubated for another 4 h. Subsequently, the supernatant was removed and cells were dissolved in 150 µl dimethyl sulfoxide (DMSO). Finally, absorbance at 570 nm was measured by using a 96-well microplate reader (Thermo Scientific).

Caspase activities assay

The activities of caspase-3 and caspase-9 were determined using the activity assay kits. To evaluate the activity of caspase, cell lysates were prepared after different treatments. Assays were performed on 96-well microtiter plates by incubating 10 µl protein of cell lysate per sample in 90 µl reaction buffer containing 10 µl caspase substrate (Ac-DEVD-pNA for caspase-3, Ac-LEHD-*p*NA for caspase-9). Lysates were incubated at 37°C for 4 h. Samples were measured with a microplate reader at an absorbance of 405 nm. The detail analysis procedure was as described in the manufacturer's protocol.

Annexin V apoptosis staining assay

Flow cytometry analysis was performed to detect early and late apoptotic cells. According to the instructions of the Annexin V and dead cell kit, cells were seeded on six-well plates at a density of 5×10^5/well. Briefly, after exposure to different treatments, the cells were harvested, washed twice with cold PBS, and resuspended in 100 µl RPMI-1640 or DMEM supplemented with 10% FBS. Then 100 µl Annexin V and dead cell reagent were added. The cells were incubated for 20 min at room temperature in the dark with gentle oscillation. The percentage of apoptotic cells was quantified with flow cytometry (Muse Cell Analyzer; Merck Millipore; Darmstadt, Germany).

Assessment of mitochondrial membrane potential ($\Delta\Psi$m)

Changes in mitochondrial membrane potential ($\Delta\Psi$m) during the early stages of apoptosis were assayed using the Muse MitoPotential kit. After being treated, cells were harvested, and the cell pellet was suspended in assay buffer (10^5 cells/100 µl). MitoPotential dye working solution was added, and the cell suspension was incubated at 37°C for 20 min. After the addition of 7-AAD dye and incubation for 5 min, changes in $\Delta\Psi$m and in cellular plasma membrane permeabilization were assessed using the fluorescence intensities of both the dyes analyzed by flow cytometry.

Western blotting

After being treated, cells were harvested and lysed in protein extraction buffer containing protease and phosphatase inhibitors. Lysed cells were centrifuged at 12,000 rpm for 15 min (at 4 °C), and the supernatant was collected to perform a Western blot analysis. Proteins were separated by gel electrophoresis in a Criterion Cell Electrophoresis System (Bio-Rad) and electroblotted onto polyvinylidene difluoride membrane (Millipore). After blocking with 5% nonfat dry milk in Tris-buffered saline (TBS) plus 0.5% Tween for 1 h, blots were incubated with primary antibodies followed by a horseradish-peroxidase-conjugated secondary antibody. The following antibodies were used: anti–Apaf-1 (1:300), anti-PARP (1:500), anti-cleaved caspase-3 (1:500), anti-cleaved caspase-9 (1:500), anti-cleaved PARP (1:500), and anti-GAPDH (1:10,000). Blots were incubated with electrochemiluminescence substrate (Thermo Fisher Scientific Inc.)

Quantitative real-time PCR for mRNA expression

Total cellular RNA was extracted from each of the experimental groups using the Qiagen miRNeasy RNA purification system according to the manufacturer's protocol. Reverse transcription was performed using gene-specific primers. Apaf-1 forward: 5′-GGAGCCATTGAGATT-3′, Apaf-1 reverse: 5′-TGAACTGGATGTGCC-3′, GAPDH forward: 5′-CCACTCCTCCACCTTTG-3′, GAPDH reverse: 5′-CACCACCCTGTTGCTGT-3′, GAPDH was taken as an internal control. Real-time PCR was performed using Platinum SYBR Green qPCR SuperMix-UDG (Invitrogen). The reactions were carried out in a 96-well optical plate at 95°C for 3 min and then amplified for 5 s at 95°C, 10 s at 56°C, followed by 25 s at 72°C for 40 cycles. The relative value of Apaf-1 expression was calculated using the $2^{-\Delta\Delta Ct}$ method. Each reverse transcription and qPCR assay was performed in triplicate.

Luciferase reporter assay

HEK293 cells were seeded in 24-well plates (1×10^5/well) and incubated until 90% confluency was reached before transfection. All transfections were carried out with Lipofectamine 2000. Cells were cotransfected with 0.5 µg pmiR-RB-Report control plasmid, pmiR-RB-Repor-Apaf-1-3′UTR wild-type or mutant reporter plasmid, 100 nmol/l miR-10b-5p mimic, or negative control. At 48 h after transfection, both firefly and renilla luciferase activities were quantified using the Dual-Luciferase reporter system (Promega) according to

the manufacturer's instructions. All experiments were performed in triplicate.

Statistical analysis

All values are expressed as mean ± SEM. SPSS 21.0 software (SPSS, Chicago, IL) was used for statistical analysis. Differences between two groups were examined for significance with the Student's *t* test. Multiple comparisons were performed with one-way analysis of variance, followed by post-hoc tests with Bonferroni's correction; *p* values of less than 0.05 were considered to be statistically significant.

ACKNOWLEDGMENTS

The present study was supported by the Natural Science Foundation of China (81302203).

REFERENCES

Becchetti A (2011). Ion channels and transporters in cancer. 1. Ion channels and cell proliferation in cancer. Am J Physiol Cell Physiol 301, C255–C265.

Bhattacharyya S, Balakathiresan NS, Dalgard C, Gutti U, Armistead D, Jozwik C, Srivastava M, Pollard HB, Biswas R (2011). Elevated miR-155 promotes inflammation in cystic fibrosis by driving hyperexpression of interleukin-8. J Biol Chem 286, 11604–11615.

Bushati N, Cohen SM (2007). microRNA functions. Annu Rev Cell Dev Biol 23, 175–205.

Charles EM, Rehm M (2014). Key regulators of apoptosis execution as biomarker candidates in melanoma. Mol Cell Oncol 1, e964037.

Chen H, Fan Y, Xu W, Chen J, Xu C, Wei X, Fang D, Feng Y (2016a). miR-10b inhibits apoptosis and promotes proliferation and invasion of endometrial cancer cells via targeting HOXB3. Cancer Biother Radiopharm 31, 225–231.

Chen W, Xia T, Wang D, Huang B, Zhao P, Wang J, Qu X, Li X (2016b). Human astrocytes secrete IL-6 to promote glioma migration and invasion through upregulation of cytomembrane MMP14. Oncotarget 7, 62425–62438.

El Fatimy R, Subramanian S, Uhlmann EJ, Krichevsky AM (2017). Genome editing reveals glioblastoma addiction to MicroRNA-10b. Mol Ther 25, 368–378.

Gabriely G, Yi M, Narayan RS, Niers JM, Wurdinger T, Imitola J, Ligon KL, Kesari S, Esau C, Stephens RM, *et al.* (2011). Human glioma growth is controlled by microRNA-10b. Cancer Res 71, 3563–3572.

Gao P, Zou Y, Zhang B, Jiang S, Hao W, Guo H, Huo G, Wang J, Zhao W, Shen B (2016). Pro-apoptotic effects of rHSG on C6 glioma cells. Int J Mol Med 38, 1190–1198.

Geiger J, Dalgaard LT (2017). Interplay of mitochondrial metabolism and microRNAs. Cell Mol Life Sci 74, 631–646.

Geng J, Liu Y, Jin Y, Tai J, Zhang J, Xiao X, Chu P, Yu Y, Wang SC, Lu J, *et al.* (2016). MicroRNA-365a-3p promotes tumor growth and metastasis in laryngeal squamous cell carcinoma. Oncol Rep 35, 2017–2026.

Huang J, Sun C, Wang S, He Q, Li D (2015). microRNA miR-10b inhibition reduces cell proliferation and promotes apoptosis in non-small cell lung cancer (NSCLC) cells. Mol Biosyst 11, 2051–2059.

Jiang X, Zhang JT, Chan HC (2012). Ion channels/transporters as epigenetic regulators? A microRNA perspective. Sci China Life Sci 55, 753–760.

Kosik KS, Krichevsky AM (2005). The elegance of the microRNAs: a neuronal perspective. Neuron 47, 779–782.

Lastraioli E, Iorio J, Arcangeli A (2015). Ion channel expression as promising cancer biomarker. Biochim Biophys Acta 1848, 2685–2702.

Li J, Li Y, Jiao J, Wang J, Li Y, Qin D, Li P (2014). Mitofusin 1 is negatively regulated by microRNA 140 in cardiomyocyte apoptosis. Mol Cell Biol 34, 1788–1799.

Li Y, Li Y, Liu J, Fan Y, Li X, Dong M, Liu H, Chen J (2016). Expression levels of microRNA-145 and microRNA-10b are associated with metastasis in non-small cell lung cancer. Cancer Biol Ther 17, 272–279.

Lin J, Teo S, Lam DH, Jeyaseelan K, Wang S (2012). MicroRNA-10b pleiotropically regulates invasion, angiogenicity and apoptosis of tumor cells resembling mesenchymal subtype of glioblastoma multiforme. Cell Death Dis 3, e398.

Liu F, Gong J, Huang W, Wang Z, Wang M, Yang J, Wu C, Wu Z, Han B (2014). MicroRNA-106b-5p boosts glioma tumorigensis by targeting multiple tumor suppressor genes. Oncogene 33, 4813–4822.

Liu Y, Li Y, Liu J, Wu Y, Zhu Q (2015). MicroRNA-132 inhibits cell growth and metastasis in osteosarcoma cell lines possibly by targeting Sox4. Int J Oncol 47, 1672–1684.

Lu FF, Wang HY, He XZ, Liang TY, Wang W, Hu HM, Wu F, Liu YW, Zhang SZ (2017). Prognostic value of ion channel genes in Chinese patients with gliomas based on mRNA expression profiling. J Neurooncol 134, 397–405.

Lu Y, Yao J, Yu J, Wei Q, Cao X (2014). The association between abnormal microRNA-10b expression and cancer risk: a meta-analysis. Sci Rep 4, 7498.

Ma L, Teruya-Feldstein J, Weinberg RA (2007). Tumour invasion and metastasis initiated by microRNA-10b in breast cancer. Nature 449, 682–688.

Martin EC, Bratton MR, Zhu Y, Rhodes LV, Tilghman SL, Collins-Burow BM, Burow ME (2012). Insulin-like growth factor-1 signaling regulates miRNA expression in MCF-7 breast cancer cell line. PLoS One 7, e49067.

Martinez R, Stuhmer W, Martin S, Schell J, Reichmann A, Rohde V, Pardo L (2015). Analysis of the expression of Kv10.1 potassium channel in patients with brain metastases and glioblastoma multiforme: impact on survival. BMC Cancer 15, 839.

Ouyang H, Gore J, Deitz S, Korc M (2014). microRNA-10b enhances pancreatic cancer cell invasion by suppressing TIP30 expression and promoting EGF and TGF-beta actions. Oncogene 33, 4664–4674.

Ru Q, Shang BY, Miao QF, Li L, Wu SY, Gao RJ, Zhen YS (2012). A cell penetrating peptide-integrated and enediyne-energized fusion protein shows potent antitumor activity. Eur J Pharm Sci 47, 781–789.

Ru Q, Tian X, Pi MS, Chen L, Yue K, Xiong Q, Ma BM, Li CY (2015). Voltage-gated K+ channel blocker quinidine inhibits proliferation and induces apoptosis by regulating expression of microRNAs in human glioma U87MG cells. Int J Oncol 46, 833–840.

Ru Q, Tian X, Wu YX, Wu RH, Pi MS, Li CY (2014). Voltage-gated and ATP-sensitive K+ channels are associated with cell proliferation and tumorigenesis of human glioma. Oncol Rep 31, 842–848.

Sand M, Skrygan M, Sand D, Georgas D, Hahn SA, Gambichler T, Altmeyer P, Bechara FG (2012). Expression of microRNAs in basal cell carcinoma. Br J Dermatol 167, 847–855.

Shen C, Gu M, Song C, Miao L, Hu L, Liang D, Zheng C (2008). The tumorigenicity diversification in human embryonic kidney 293 cell line cultured in vitro. Biologicals 36, 263–268.

Shen X, Li J, Liao W, Wang J, Chen H, Yao Y, Liu H, Ding K (2016). microRNA-149 targets caspase-2 in glioma progression. Oncotarget 7, 26388–26399.

Spitzner M, Ousingsawat J, Scheidt K, Kunzelmann K, Schreiber R (2007). Voltage-gated K+ channels support proliferation of colonic carcinoma cells. FASEB J 21, 35–44.

Teplyuk NM, Uhlmann EJ, Gabriely G, Volfovsky N, Wang Y, Teng J, Karmali P, Marcusson E, Peter M, Mohan A, *et al.* (2016). Therapeutic potential of targeting microRNA-10b in established intracranial glioblastoma: first steps toward the clinic. EMBO Mol Med 8, 268–287.

Teplyuk NM, Uhlmann EJ, Wong AH, Karmali P, Basu M, Gabriely G, Jain A, Wang Y, Chiocca EA, Stephens R, *et al.* (2015). MicroRNA-10b inhibition reduces E2F1-mediated transcription and miR-15/16 activity in glioblastoma. Oncotarget 6, 3770–3783.

Thompson EG, Sontheimer H (2016). A role for ion channels in perivascular glioma invasion. Eur Biophys J 45, 635–648.

Visone R, Croce CM (2009). MiRNAs and cancer. Am J Pathol 174, 1131–1138.

Voloboueva LA, Giffard RG (2011). Inflammation, mitochondria, and the inhibition of adult neurogenesis. J Neurosci Res 89, 1989–1996.

Xue H, Guo X, Han X, Yan S, Zhang J, Xu S, Li T, Guo X, Zhang P, Gao X, *et al.* (2016). MicroRNA-584–3p, a novel tumor suppressor and prognostic marker, reduces the migration and invasion of human glioma cells by targeting hypoxia-induced ROCK1. Oncotarget 7, 4785–4805.

Zhang Y, Yang L, Gao YF, Fan ZM, Cai XY, Liu MY, Guo XR, Gao CL, Xia ZK (2013). MicroRNA-106b induces mitochondrial dysfunction and insulin resistance in C2C12 myotubes by targeting mitofusin-2. Mol Cell Endocrinol 381, 230–240.